REPORT DOCUMENTATION PAGE

Form Approved
OMB No. 0704-0188

1. REPORT DATE *(DD-MM-YYYY)*
December 2013

2. REPORT TYPE
Viewgraph

3. DATES COVERED *(From - To)*
December 2013- January 2014

4. TITLE AND SUBTITLE
Development of a Facility for Combustion Stability Experiments at Supercritical Pressure

5a. CONTRACT NUMBER
In-House

5b. GRANT NUMBER

5c. PROGRAM ELEMENT NUMBER

6. AUTHOR(S)
Wegener, Leyva, Forliti, Talley

5d. PROJECT NUMBER

5e. TASK NUMBER

5f. WORK UNIT NUMBER
Q0YA

7. PERFORMING ORGANIZATION NAME(S) AND ADDRESS(ES)

Air Force Research Laboratory (AFMC)
AFRL/RQRC
10 E. Saturn Blvd
Edwards AFB CA 93524-7680

8. PERFORMING ORGANIZATION REPORT NO.

9. SPONSORING / MONITORING AGENCY NAME(S) AND ADDRESS(ES)
Air Force Research Laboratory (AFMC)
AFRL/RQR
5 Pollux Drive
Edwards AFB CA 93524-7048

10. SPONSOR/MONITOR'S ACRONYM(S)

11. SPONSOR/MONITOR'S REPORT NUMBER(S)
AFRL-RQ-ED-VG-2013-281

12. DISTRIBUTION / AVAILABILITY STATEMENT
Distribution A: Approved for Public Release; Distribution Unlimited. PA#13562

13. SUPPLEMENTARY NOTES
Viewgraph for the 52nd AIAA Aerospace Sciences Meeting, National Harbour, MD, 13 January 2013

14. ABSTRACT
Combustion instability in liquid rocket engines can have severe consequences including degraded performance, accelerated component wear, and potentially catastrophic failure. High-frequency instabilities, which are generally the most harmful in liquid rocket engines, can be driven by interactions between disturbances associated with transverse acoustic resonances and the combustion process. The combustion response to acoustic perturbation is a critical component of the instability mechanism, and is in general not well understood. The current paper describes an experimental facility at the Air Force Research Laboratory (AFRL) at Edwards Air Force Base that is intended to investigate the coupling between transverse acoustic resonances and single/multiple liquid rocket engine injector flames. Critical aspects of the facility will be described, including the capability to operate at supercritical pressures that are relevant to high-performance liquid rocket engines, accurately-controlled and cryogenically-conditioned propellants, and optical access to facilitate the use of advanced diagnostics. The transverse acoustic resonance is induced through the use of carefully-controlled piezo-sirens, allowing monochromatic excitation across a range of amplitudes at a number of discrete frequencies. The location of the flame within the acoustic resonance mode shape can also be varied through relative phase control of the two acoustic sources. The operating space of the facility, for oxygen and hydrogen operation, will be described. Preliminary non-reacting and reacting data will also be presented to demonstrate the quality of operation of this facility. It is anticipated that future results generated using this facility will provide both fundamental insight into the acoustic-flame interactions as well as provide a database useful for validating combustion instability models.

15. SUBJECT TERMS

16. SECURITY CLASSIFICATION OF:			17. LIMITATION OF ABSTRACT	18. NUMBER OF PAGES	19a. NAME OF RESPONSIBLE PERSON
					Doug Talley
a. REPORT	**b. ABSTRACT**	**c. THIS PAGE**	SAR	31	**19b. TELEPHONE NO** *(include area code)*
Unclassified	**Unclassified**	**Unclassified**			661-525-6174

Standard Form 298 (Rev. 8-98)
Prescribed by ANSI Std. 239.18

Development of a Facility for Combustion Stability Experiments at Supercritical Pressure

Jeff Wegener, Ivett Leyva, David Forliti, and Doug Talley
Air Force Research Laboratory
Combustion Devices Branch - Combustion Stability Group
Edwards AFB, California

Supported by
Air Force Office Scientific Research
Air Force Research Laboratory

Overview

- Background
    - Combustion Instability
    - Challenges
- Experimental Techniques
    - Facility
        - Heat Exchangers
        - Acoustic Excitation System
        - Injector
    - Proper Orthogonal Decomposition of High-speed Images
- Preliminary Results

Background

- Liquid Rocket Engine Combustion Instability

Motivation

–An organized, oscillatory motion in the combustion chamber sustained by combustion

–Chamber pressure amplitudes p' can exceed 100% of the mean chamber pressure p_c

–Most difficult instabilities to eliminate:

high frequency (a.k.a. "screaming" instability)

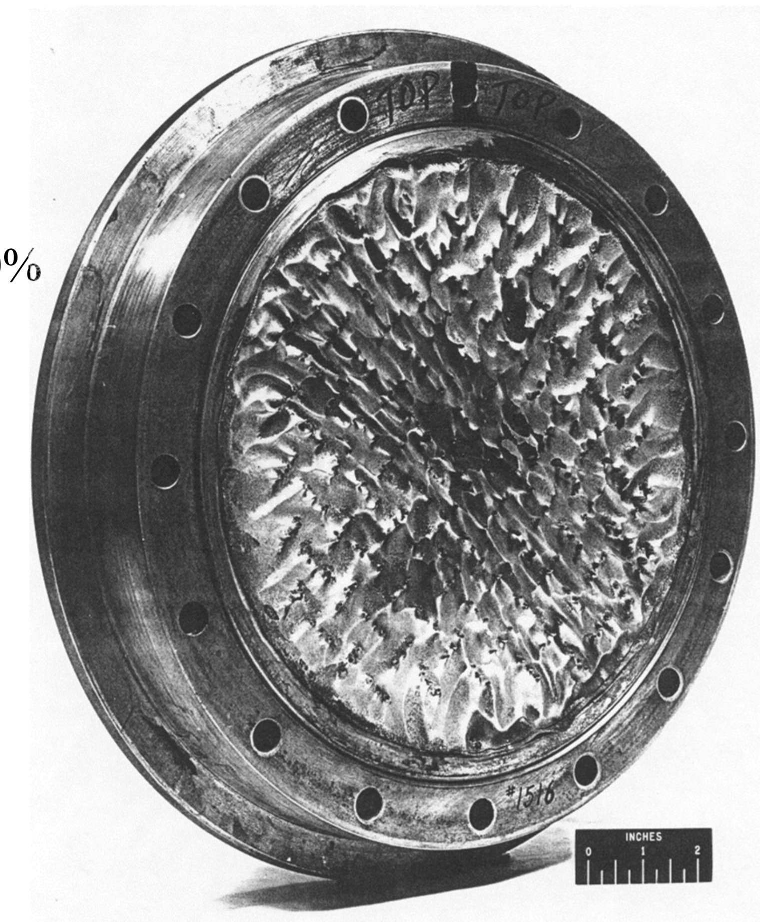

Irreparable damage can occur in < 1s

Background

- Combustion Instability Feedback Loop

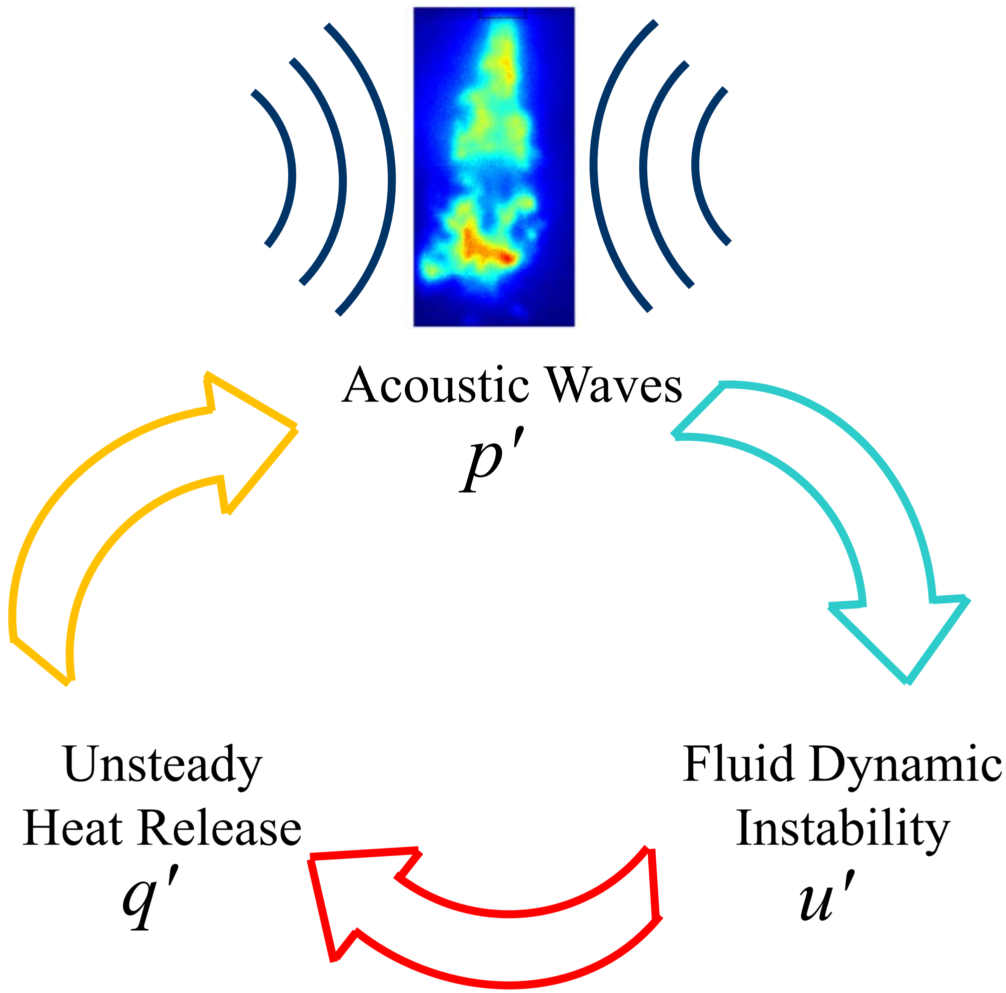

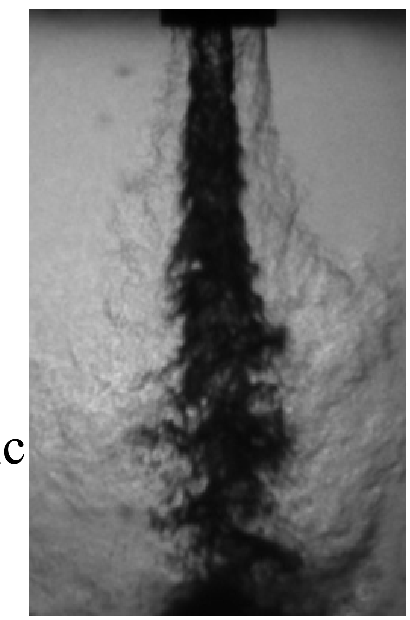

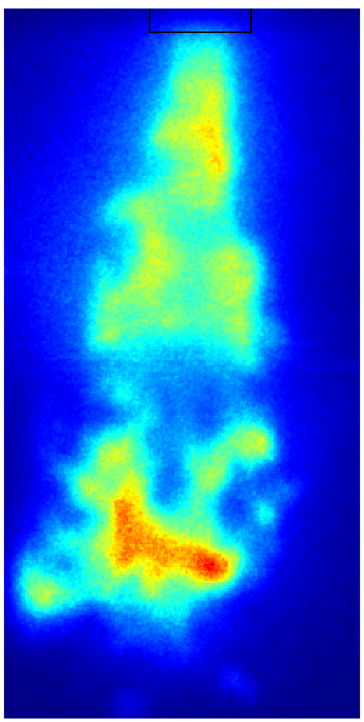

OH* Chemiluminescence of an H_2/O_2 flame (from present reactive experiments)

Background

Reactive

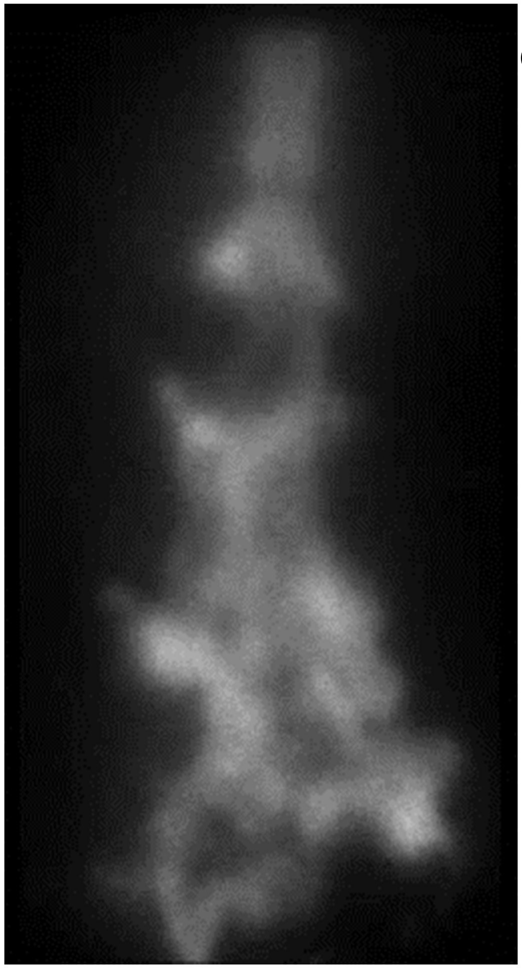

OH* Chemiluminescence
Coaxial O_2-H_2 Flame
$p_c = 400$ psia

Coaxial Injector
Cross-sectional View

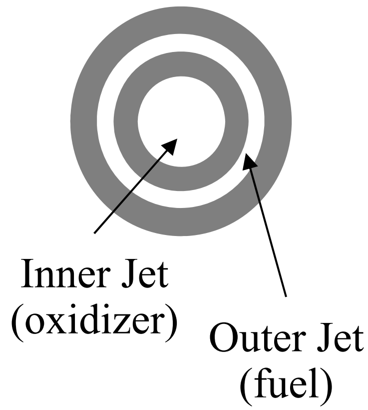

Density Ratio

$$S = \rho_{oj}/\rho_{ij}$$

Velocity Ratio

$$R = u_{oj}/u_{ij}$$

Momentum Flux Ratio

$$J = SR^2$$

Nonreactive

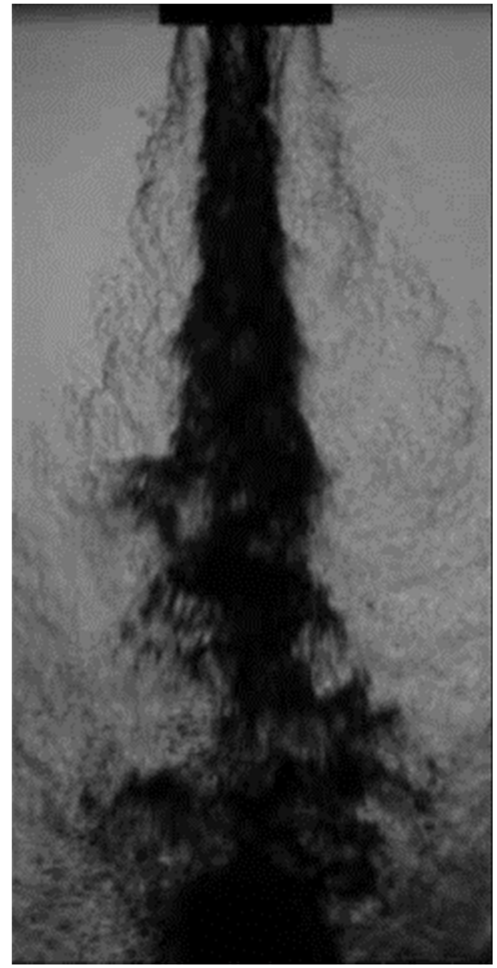

Back-lit Imaging
Coaxial LN_2-GHe Jet
$p_c = 400$ psia

Background

- Shear-Coaxial Jet Flow Diagram

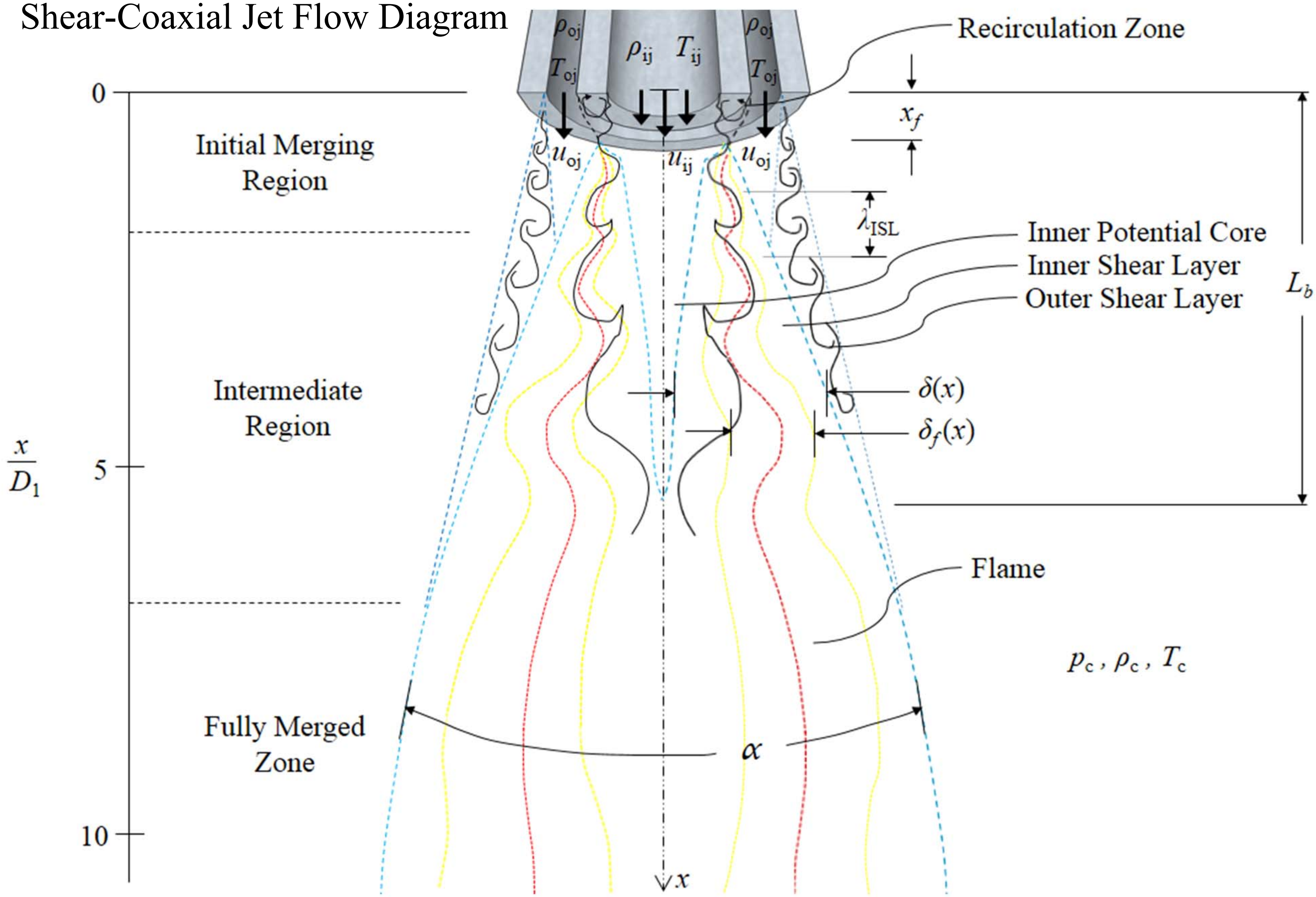

Background:
Challenges Associated with Combustion Stability Experimental Facilities

- Supercritical Chamber Pressure
  - Liquid rocket engines (LREs) often employ chamber pressures greater than the critical pressure of oxygen

    $p_c > 731$ psia
  - Surface tension and phase changes are undefined
- High Amplitude Acoustic Perturbations
  - Severe LRE combustion instabilities involve pressure amplitudes far greater than those of traditional acoustic excitation systems ($p' \sim p_c$)
- Imaging Diagnostics
  - High-speed (>10 kHz) optical equipment is required to capture unsteady heat release via chemiluminescence and planar laser induced fluorescence (PLIF)
  - Windows must endure large changes in temperature as well as high chamber pressures

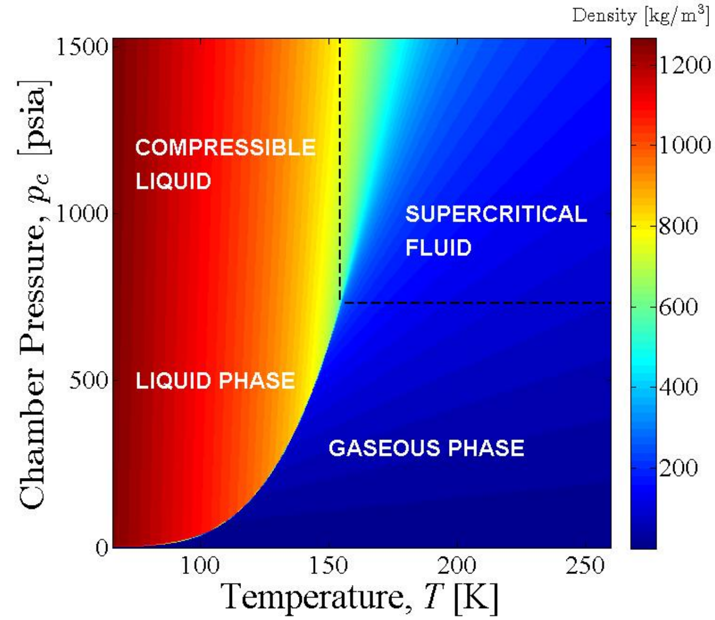

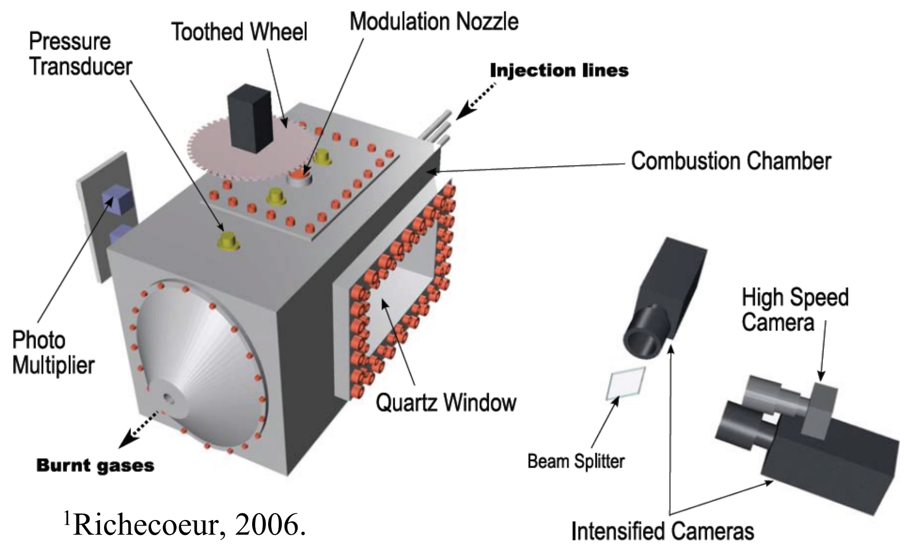

[1]Richecoeur, 2006.

Existing Facilities

DLR (Germany)	CNRS (France)
Purdue Univ.	Penn. State Univ.

Experimental Techniques: Facility

- Capabilities
  - Cryogenic propellant temperature control with high accuracy (±1 K)
  - Sub- and super-critical chamber pressure (p_c up to 10.4 MPa)
  - High amplitude acoustic forcing ($p'/p_c \sim 0.02$)
  - Coaxial injector with extended length for fully developed turbulent flow
  - High speed diagnostic tools
    - Pressure transducer(s) natural frequency > 100 kHz
    - Time-series OH* chemiluminescence imaging (f > 10 kHz)

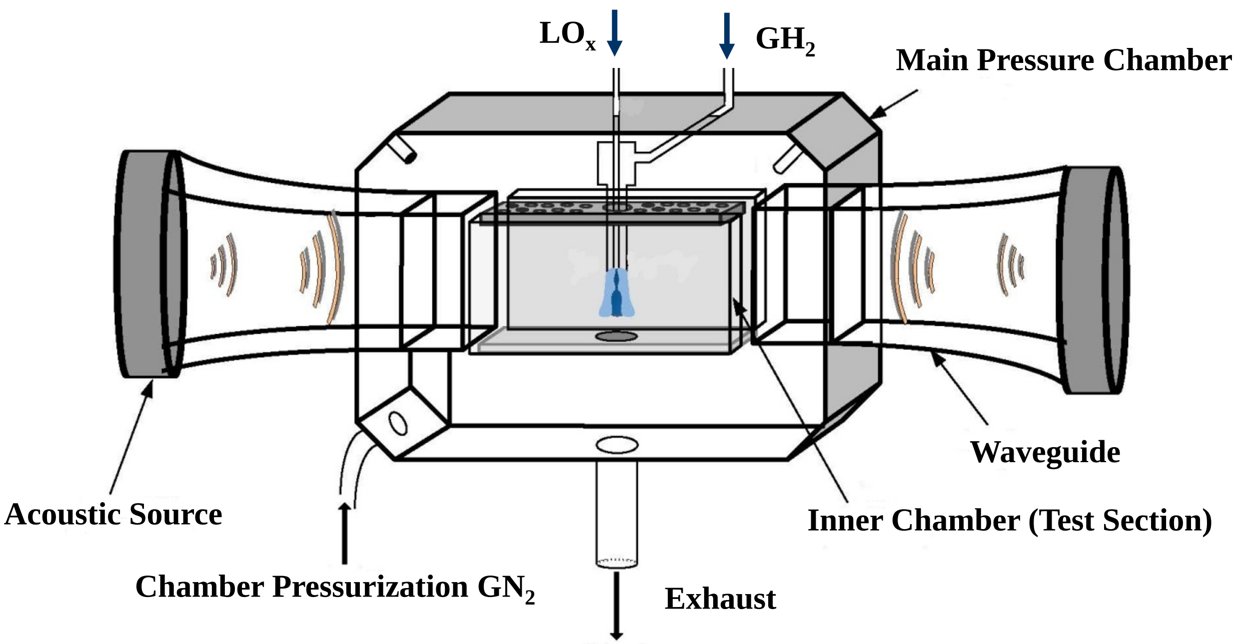

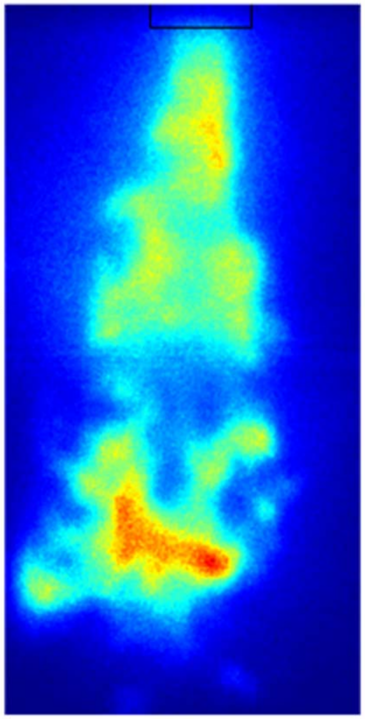

OH* Chemiluminescence of an H_2/O_2 flame (from present reactive experiments)

Experimental Techniques: Facility

BEFORE

2011

AFTER

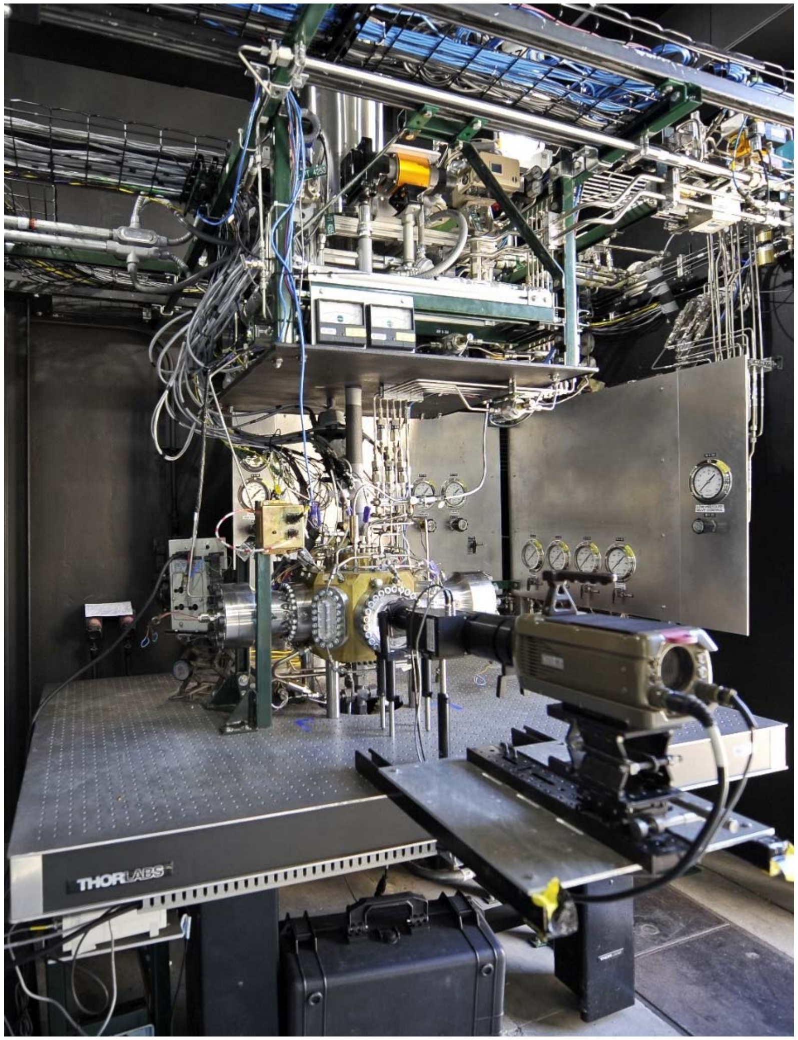

2013

DISTRIBUTION A. Approved for public release; distribution unlimited

Experimental Techniques: Facility

BEFORE

2011

AFTER

2013

Experimental Techniques: Heat Exchangers

- Heat Exchanger Design Objectives
  - Achieve inner and outer jet temperatures, T_{ij} and T_{oj}, which are similar to the propellant temperatures of a liquid rocket engine
  - Minimize: temperature control error, coolant flow rate, user interaction

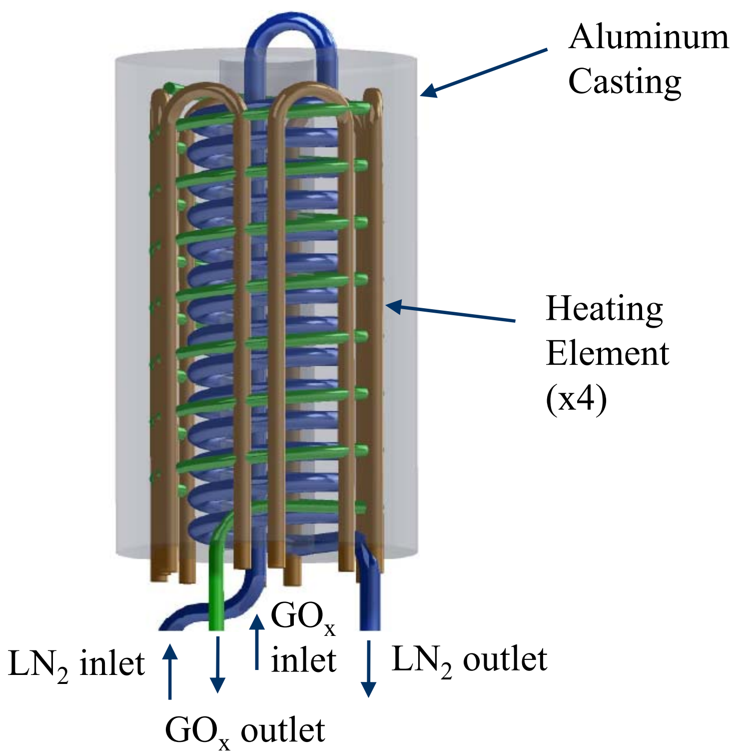

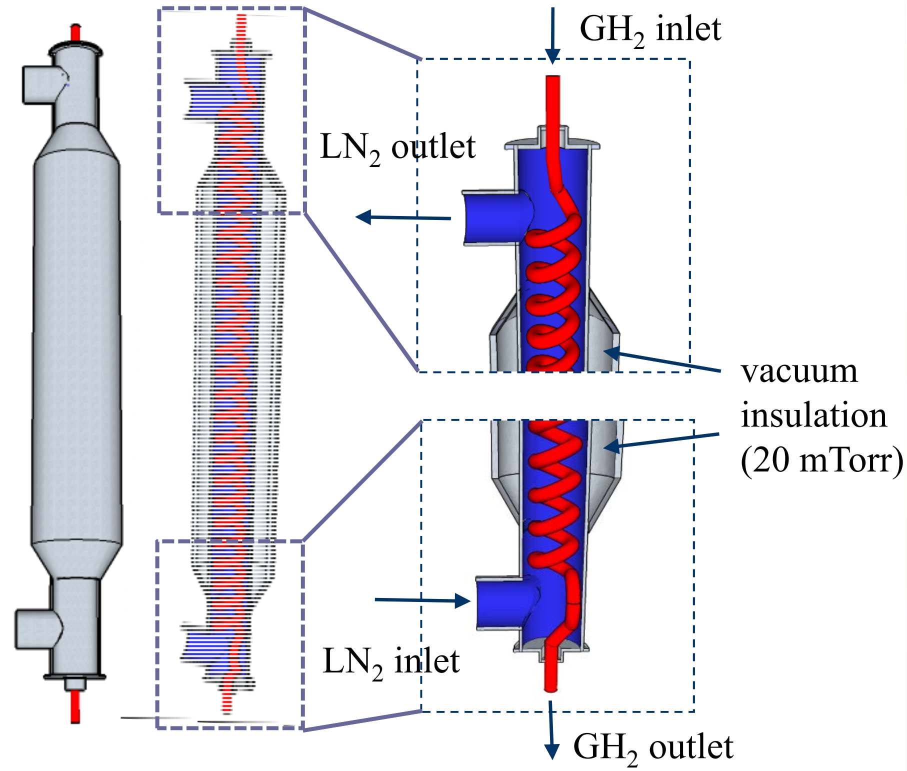

Experimental Techniques: Heat Exchangers

- Inner Jet Heat Exchanger

(data collected using oxygen)

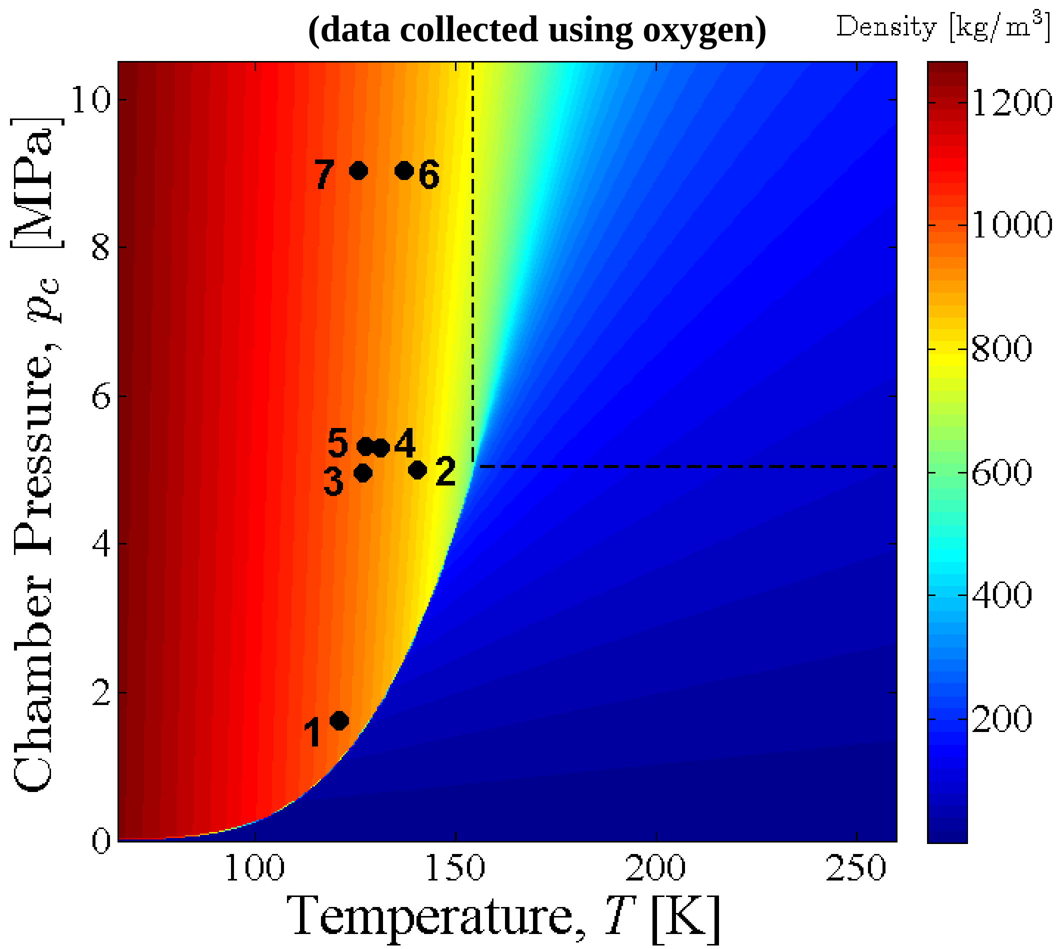

	$\dot{m}_{ij}$
• **1**	3.7 g/s
• **2**	2.6 g/s
• **3**	9.3 g/s
• **4**	3.0 g/s
• **5**	11.1 g/s
• **6**	2.7 g/s
• **7**	10.4 g/s

Both gaseous oxygen and liquid oxygen conditions can be achieved.

Inner jet mass flow rate has a significant effect on inner jet temperature.

Pressure has a negligible effect on inner jet temperature.

Experimental Techniques: Waveguides

- Objective: To create an acoustic field with a **transverse standing wave**.

Velocity Node: $L = n\lambda = n\dfrac{c}{f_n}$ Pressure Node: $L = \left(\dfrac{2n+1}{2}\right)\lambda = \left(\dfrac{2n+1}{2}\right)\dfrac{c}{f_n}$

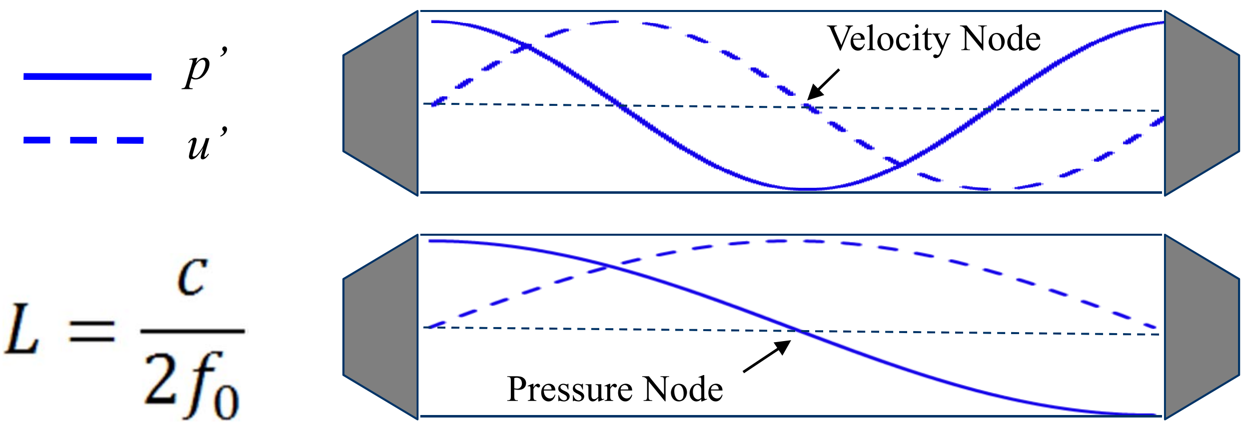

$\phi = 0°$

$L = \dfrac{c}{2f_0}$

$\phi = 180°$

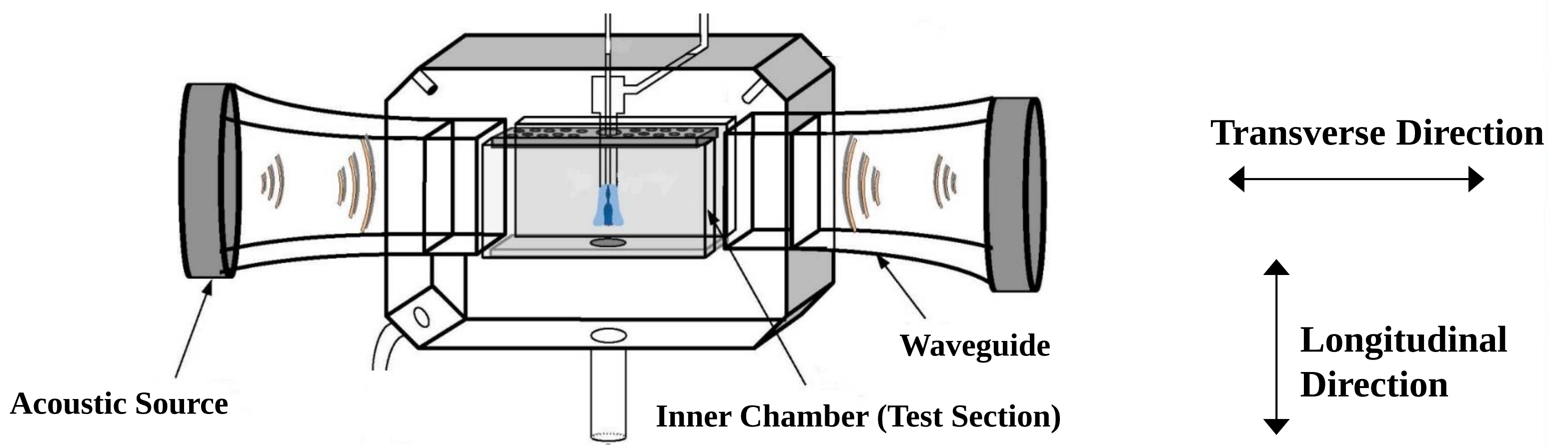

Experimental Techniques: Waveguides

- Acoustic Waveguide Design
  - Objectives
    - Minimize: two- and three-dimensional waves
    - Maximize: pressure amplitude
  - Derivation of area relation
    - Webster's horn equation

$$\frac{1}{A}\frac{\partial}{\partial y}\left(A\frac{\partial p}{\partial y}\right)-\frac{1}{c^2}\frac{\partial^2 p}{\partial t^2}=0$$ [11]

- General solution for area

$$A^{1/2}=A_{th}^{1/2}(\cosh my+T\sinh my)$$

where $A=A_{th}(\cosh my)^2$ and $A_{th}^{1/2}Tm=\frac{\partial(A^{1/2})}{\partial y}(y=0)$

- Particular solution for the catenoidal horn ($T=0$)

$$* \quad A=A_{th}(\cosh my)^2$$

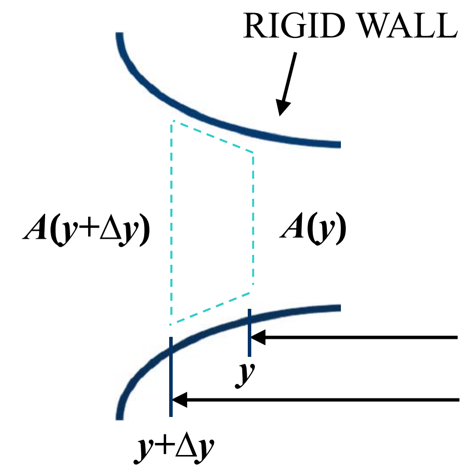

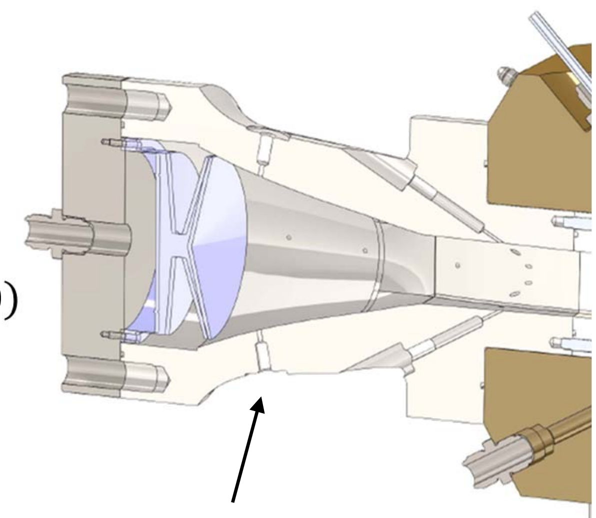

WAVEGUIDE CAD CROSS-SECTION

[2] Pierce, A. D., Acoustics: An Introduction to Its Physical Principles and Applications, 2nd Edition, 360-363, 1991.

Experimental Techniques: Waveguides

- Acoustic Characterization: Piezoelectric sirens placed *outside* of the chamber at ambient pressure

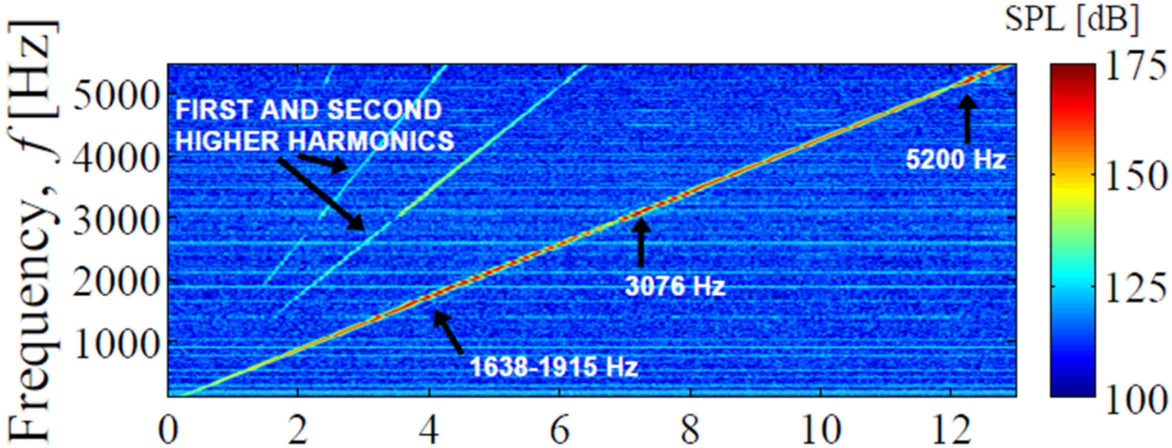

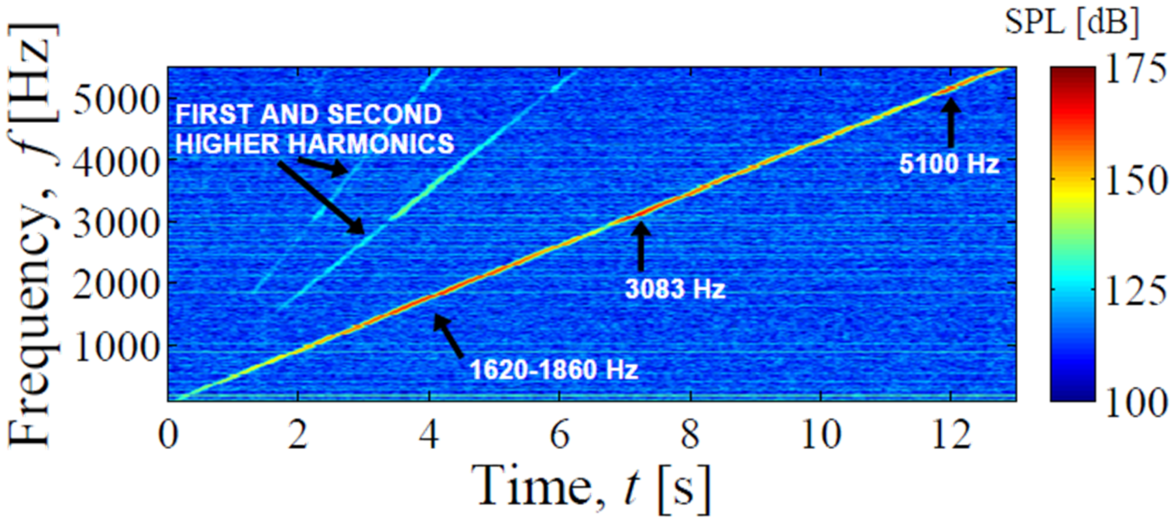

PIEZOELECTRIC SIREN

⇨ Each siren has a unique frequency response, with 3 peak frequency bands.

Experimental Techniques: Waveguides

- Acoustic Characterization: Piezoelectric sirens operated in-phase at p_c = 400 psia

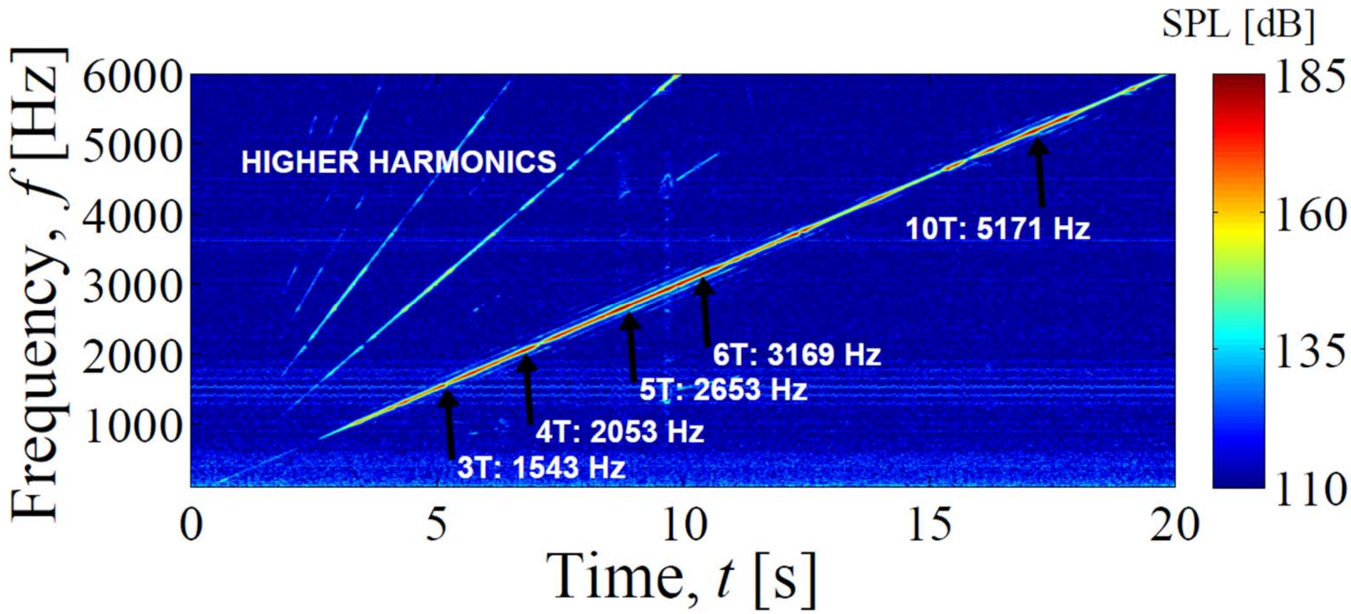

Several transverse modes can be identified.

- Conclusions
  - An array of transverse modes will produce high amplitudes (3T, 4T, 5T, 6T, 10T modes).
  - Operating at other frequencies produces either low amplitudes, or undesired resonance, e.g. longitudinal resonance.
  - Peak frequency values are dependent on chamber pressure and temperature
  - → Standing waves must be verified prior to each individual experimental test.

Experimental Techniques: Injector

Objective: create a LO_x/GH_2 injector which provides fully turbulent exit flow

Challenges

- Materials
- Robust separation between GH_2 and LO_x
- Large injector length ($l_e/D \geq 4.4\mathrm{Re}^{1/6}$ for fully developed turbulent flow[9])
- Small cross sectional size
- Rigidity
- Manufacturability

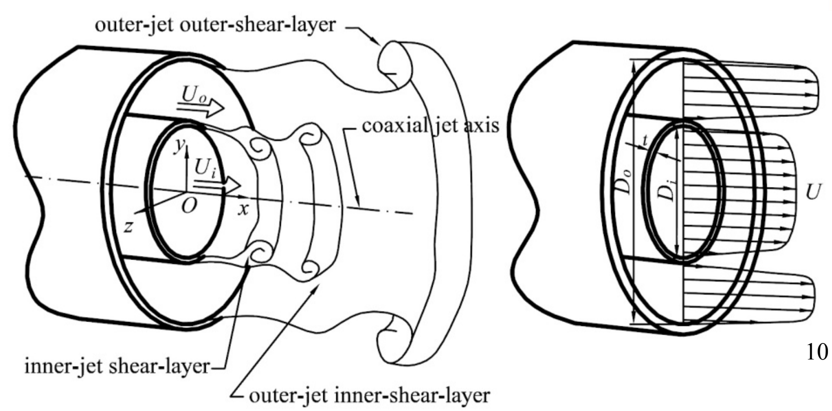

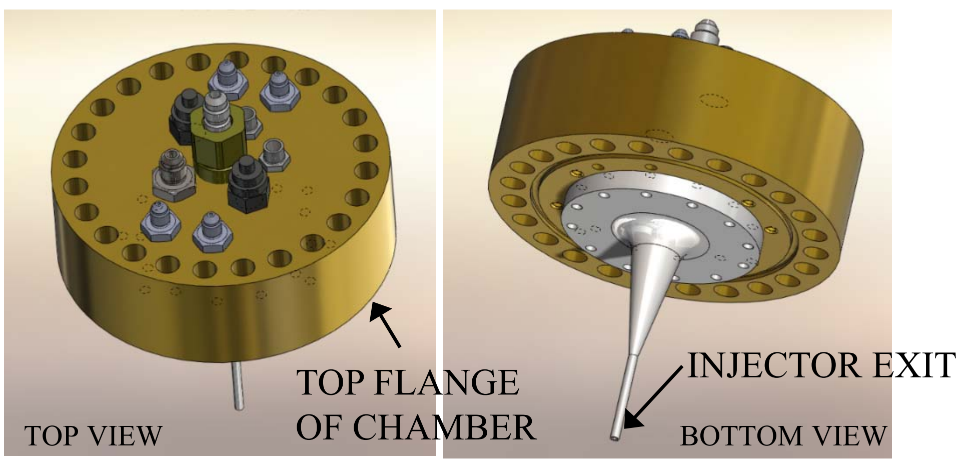

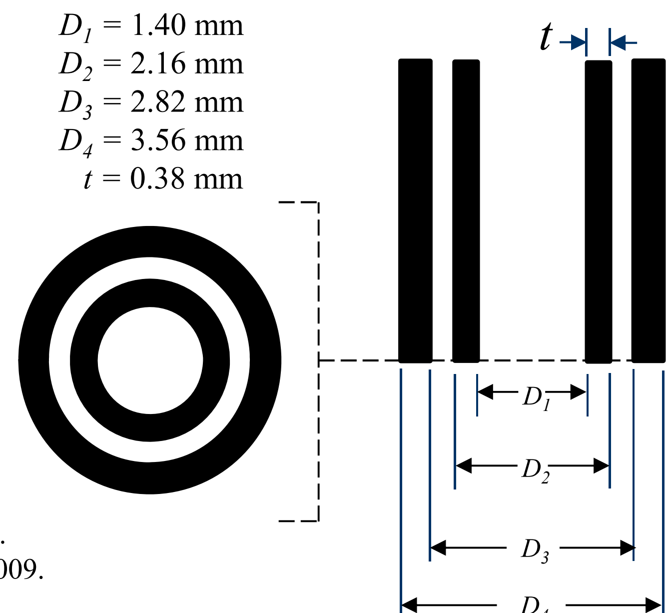

[3] Munson, B. R., Young, D. F., Okiishi, T. H., Fundamental Fluid Mechanics, 5th Edition, 2005.
[4] Burattini, P. and Talamelli, A., "Acoustic control of a coaxial jet," J. of Turbulence, 8, 1-14, 2009.

Experimental Techniques: Image Analysis

- Proper Orthogonal Decomposition
  - For a set of high-speed images,

$$\boldsymbol{A} = \sum_{k=1}^{N} q_k(t)\varphi_k(x)$$

$\boldsymbol{A}$: pixel intensity data matrix
q_k: vectors of temporal amplitude coefficients
φ_k: vectors of proper orthogonal modes
k : mode number
N : total number of modes

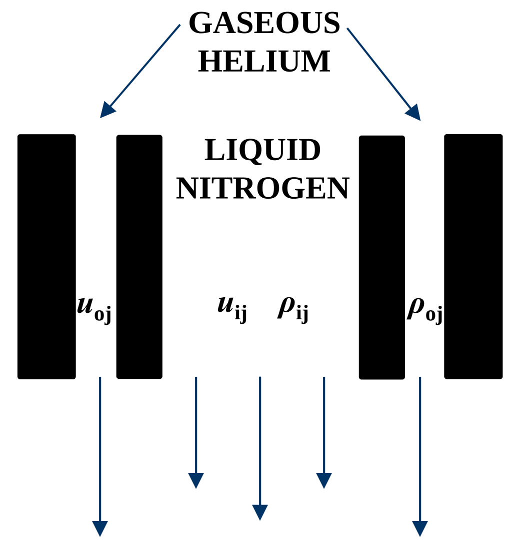

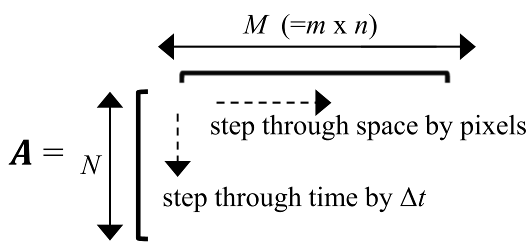

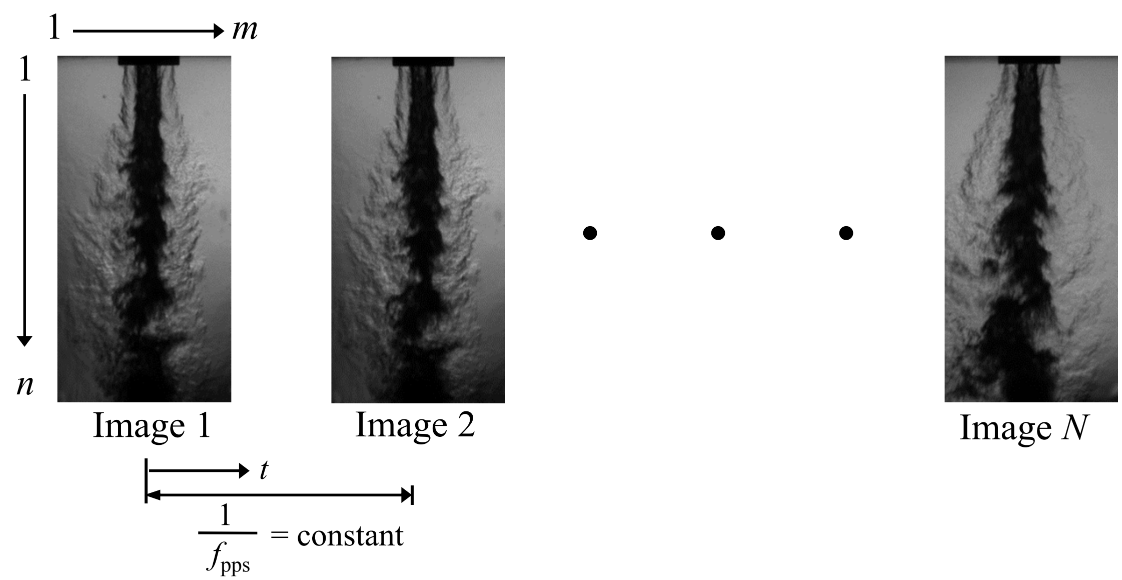

Experimental Techniques: Image Analysis

- Proper Orthogonal Decomposition
  - To identify periodic structures, subtract the average image

$$\tilde{\boldsymbol{A}}_{ij} = \boldsymbol{A}_{ij} - \frac{1}{N}\sum_i \boldsymbol{A}_{ij} \qquad i = 1\ldots N, \quad j = 1\ldots M$$

$\tilde{\boldsymbol{A}}$: matrix of intensity fluctuations

- Singular Value Decomposition (SVD) of $\tilde{\boldsymbol{A}}$

$$\tilde{\boldsymbol{A}} = \tilde{\boldsymbol{U}}\Sigma \boldsymbol{V}^{\boldsymbol{T}}$$

equivalent to $q_k(t)$ equivalent to $\varphi_k(x)$

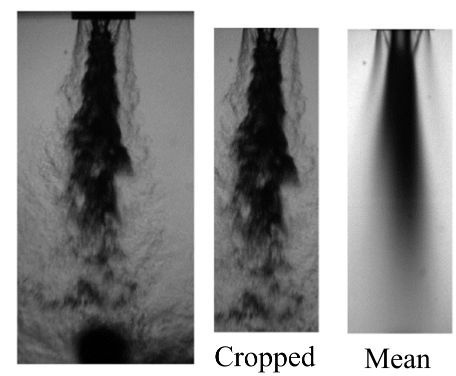

Snapshot Image Cropped Mean

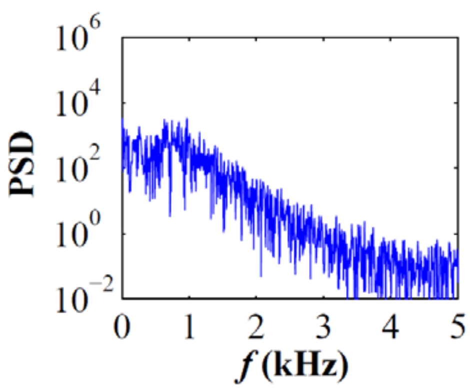

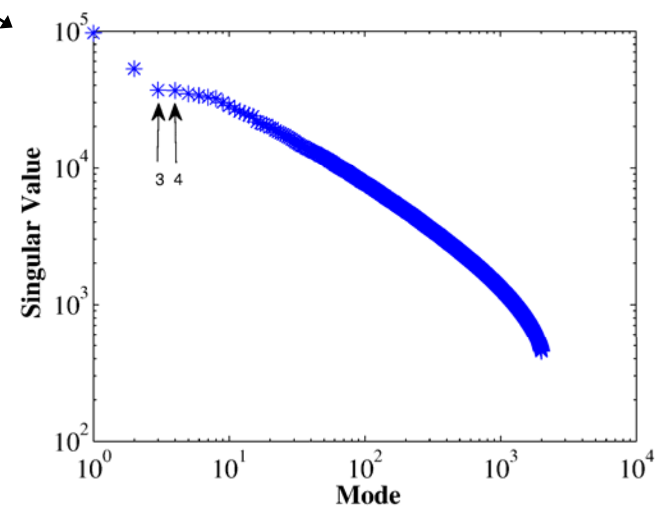

POM 3

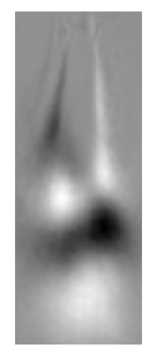

p_c = **400 psia**
J = **6**

Experimental Techniques: Image Analysis

- Proper Orthogonal Decomposition
  - To identify traveling, coherent structures, a conjugate mode pair is identified as any two modes whose CPSD magnitude peaks near a phase of ±90°.[5]

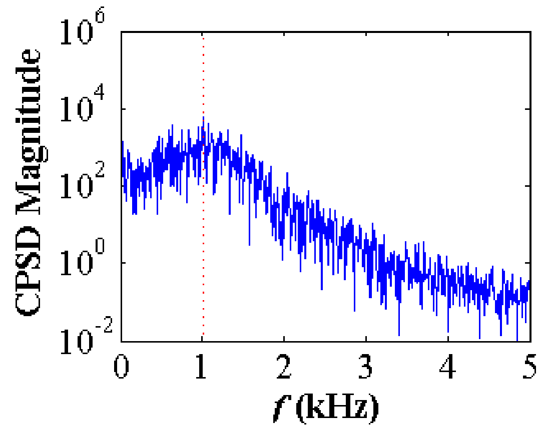

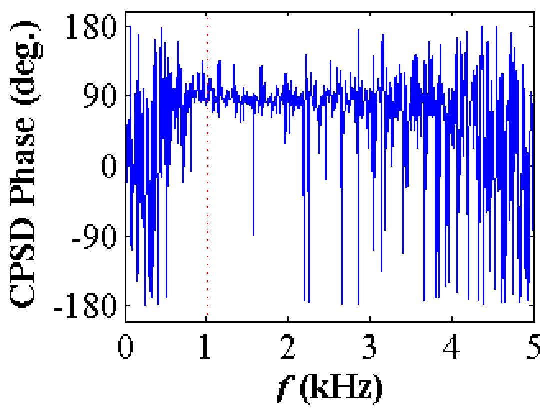

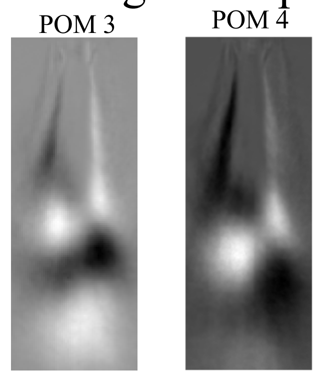

POMs 3 & 4 exhibit the same flow structure, shifted by 90° in the direction of flow.

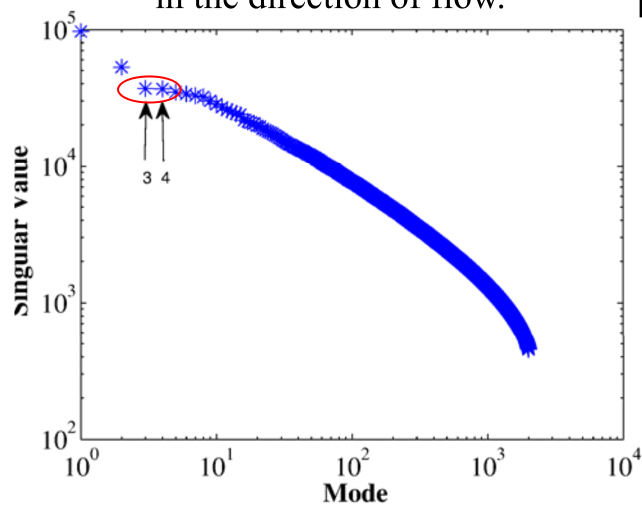

⇨ Proper orthogonal modes (POMs) 3 & 4 were found to be the **most energetic conjugate pair.**

⇨ The natural mode is represented by POMs 3 & 4.

⇨ The natural mode spans a band of frequencies rather than a single peak frequency.

Results: Unforced Coaxial Jets

- Natural Jet Characterization: f_{nat} values determined by POD

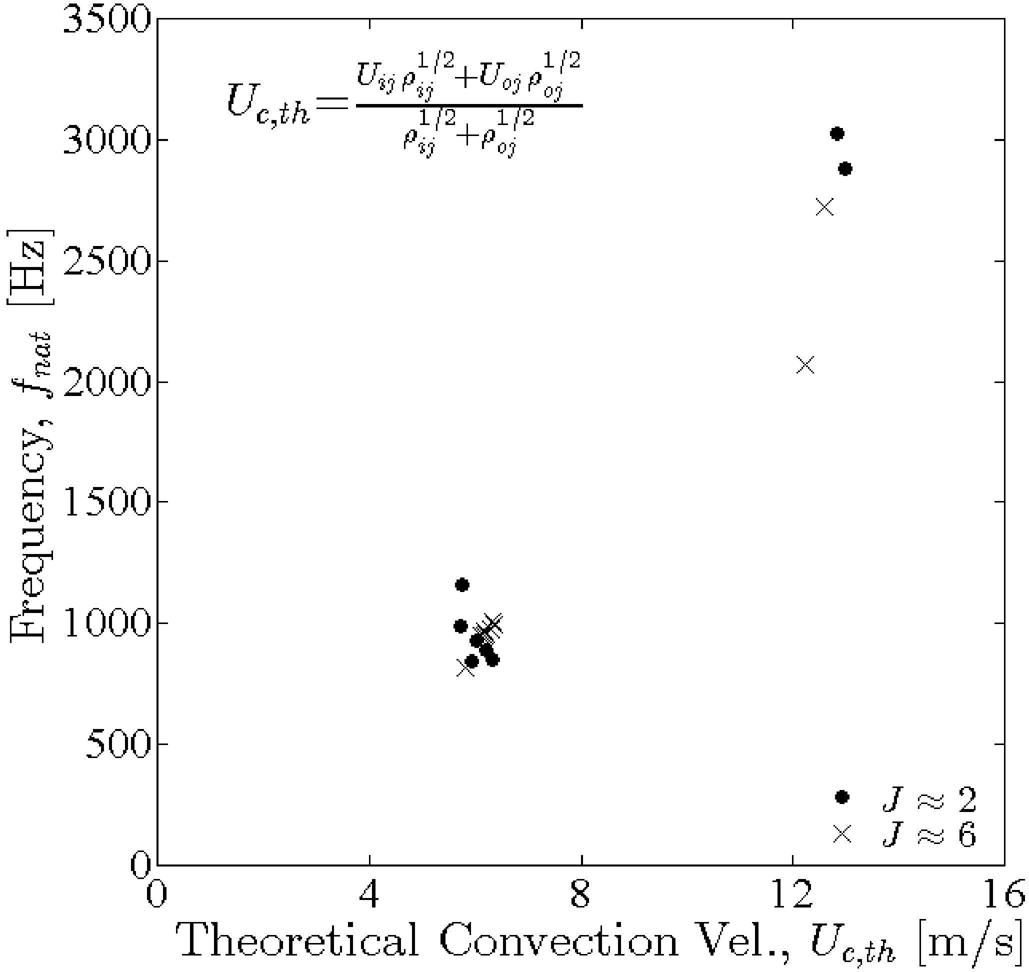

- Inner jet: LN_2
- Outer jet: GHe
- Two $U_{c,th}$ values are used
- Two J values are used
- p_c = 400 psia

⇨ f_{nat} scales with $U_{c,th}$ **approximately**

[6] Dimotakis, P. E. 1986 "Two-Dimensional Shear-Layer Entrainment," *AIAA J.* 24, 1791-1796.

Results: Unforced Coaxial Jets

- High-speed images were used to **experimentally measure** the shear layer convection velocity

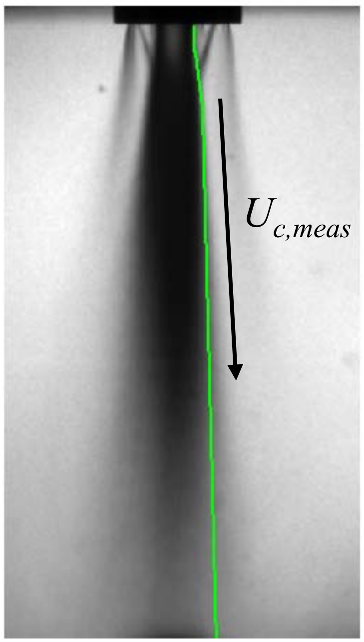

$$U_{c,meas} = \frac{\Delta s}{\Delta t}$$

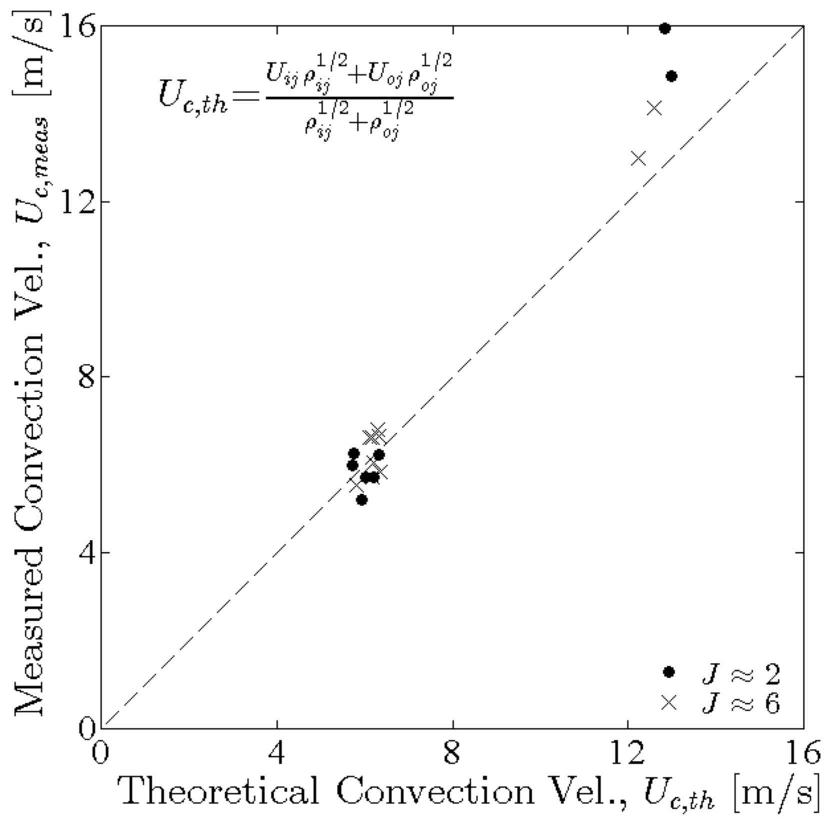

⇨ $U_{c,th}$ accurately predicts convection velocities near 6 m/s

⇨ $U_{c,th}$ under-predicts higher convection velocities

Results: Unforced Coaxial Jets

- Natural Jet Characterization: *St* scaling law produced by **experimental** shear layer convection velocities

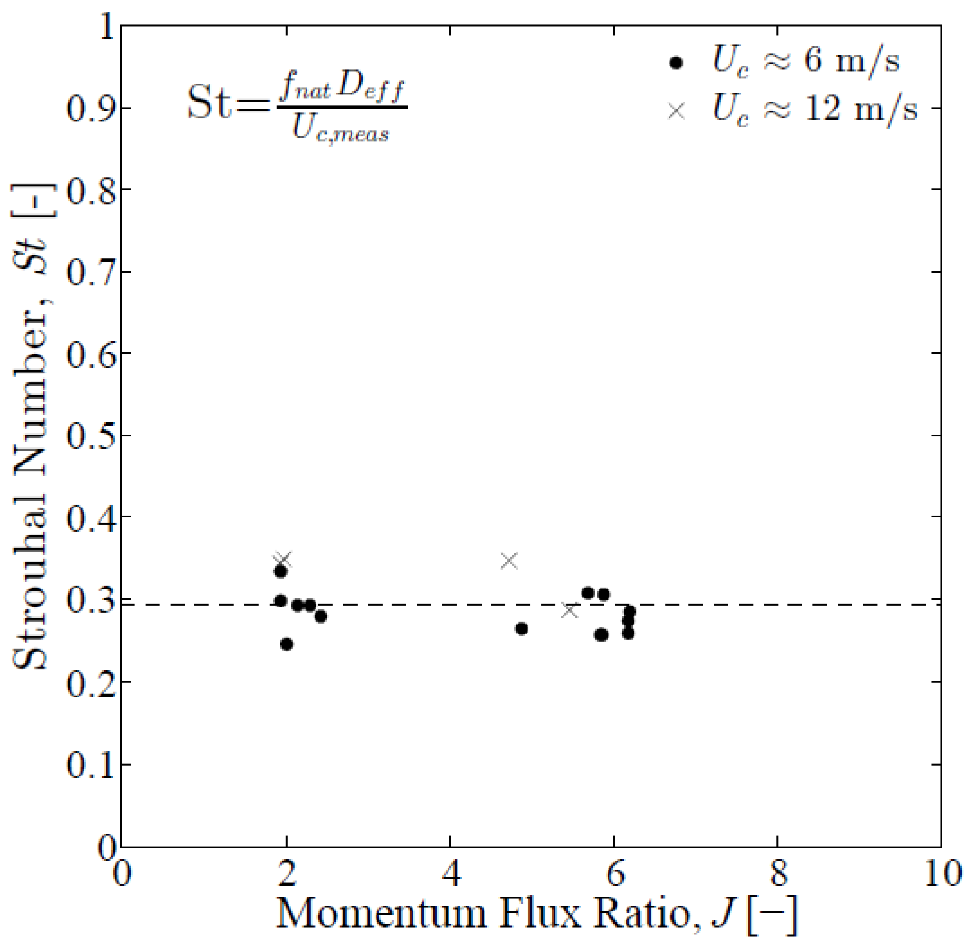

- $D_{eff} = \dfrac{D_1 + D_2}{2}$

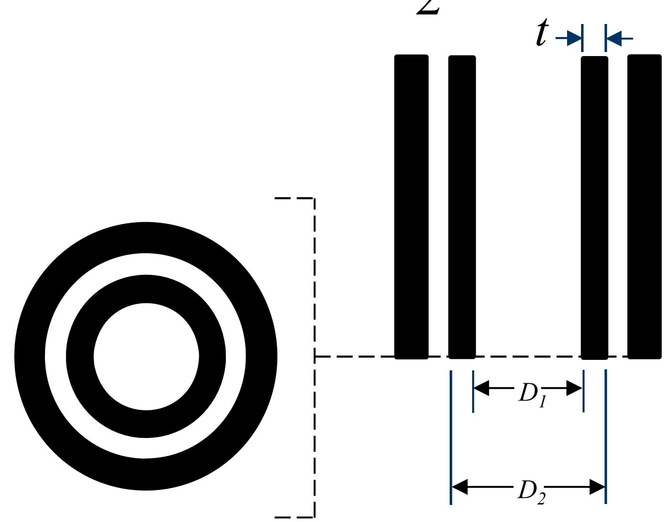

⇨ *St* values collapse around a mean of 0.29

⇨ *St* is not dependent on *J*

Future Work

- Nonreactive Experiments
  - Explore susceptibility of jets to acoustic forcing with regard to:
    - Nondimensional Forcing Frequency $F = f_F/f_{\mathrm{nat}}$
    - Acoustic pressure amplitude p'
    - Momentum Flux Ratio J
    - Injector Geometry $AR = A_{oj}/A_{ij}$
  - Explore the existence of convectively unstable and absolutely unstable coaxial jets

Non-reactive

- Reactive Experiments
  - Characterize the spectral content of natural flame instabilities
  - Explore hydrogen and hydrocarbon fuels
  - Explore variations in injector geometry, including gas-centered swirl-coaxial injectors

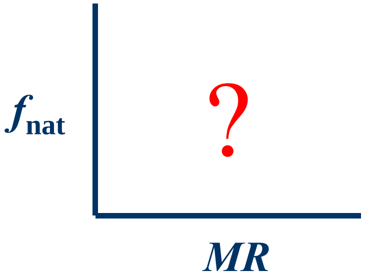

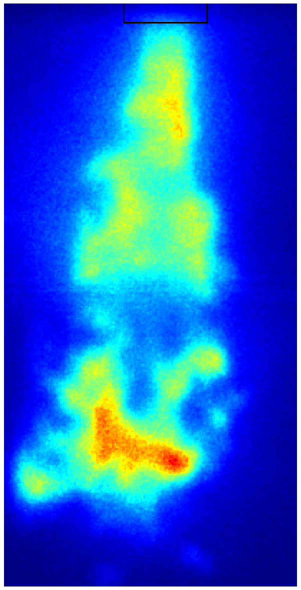

Reactive

DISTRIBUTION A. Approved for public release; distribution unlimited

Summary

- A facility for combustion stability experiments was constructed to allow for chamber pressures up to 1500 psi and acoustic pressure amplitudes greater than 2% of the mean chamber pressure.

- Cryogenic heat exchangers were characterized as an effective technique to control the temperature of both oxygen and hydrogen at the injector.

- A shear-coaxial injector was designed and fabricated to produce fully developed turbulence at the exit for a wide range of Re.

- Preliminary, nonreactive results were analyzed using proper orthogonal decomposition of high-speed images to extract the dominant instability frequency of each flow condition.

- Future work will characterize the spectral behavior of reactive coaxial jets with regard to fuel type and injector geometry, and study the susceptibility of these flows to transverse acoustic forcing.

References

1. Richecoeur, F., “Experiments and numerical simulations of interactions between transverse acoustic modes and cryogenic flames,” PhD thesis, Ecole Centrale Paris, November 2006.
2. Pierce, A. D., Acoustics: An Introduction to Its Physical Principles and Applications, 2nd Edition, 360-363, 1991.
3. Munson, B. R., Young, D. F., Okiishi, T. H., Fundamental Fluid Mechanics, 5th Edition, 2005.
4. Burattini, P. and Talamelli, A., “Acoustic control of a coaxial jet,” J. of Turbulence, 8, 1-14, 2009.
5. Arienti, M. and Soteriou, M.C., “Time resolved proper orthogonal decomposition of liquid jet dynamics,” *Phys of Fluids*, 21 112104, 2009.
6. Dimotakis, P. E. "Two-Dimensional Shear-Layer Entrainment," *AIAA* 24, 1791-1796, 1986.

Experimental Techniques: Facility

- OH* Chemiluminescence Imaging
  - Radiative de-excitation of hydroxyl radicals emits ultraviolet light at a wavelength of approximately 308 nm.

$$OH^* \longrightarrow OH + h\nu$$

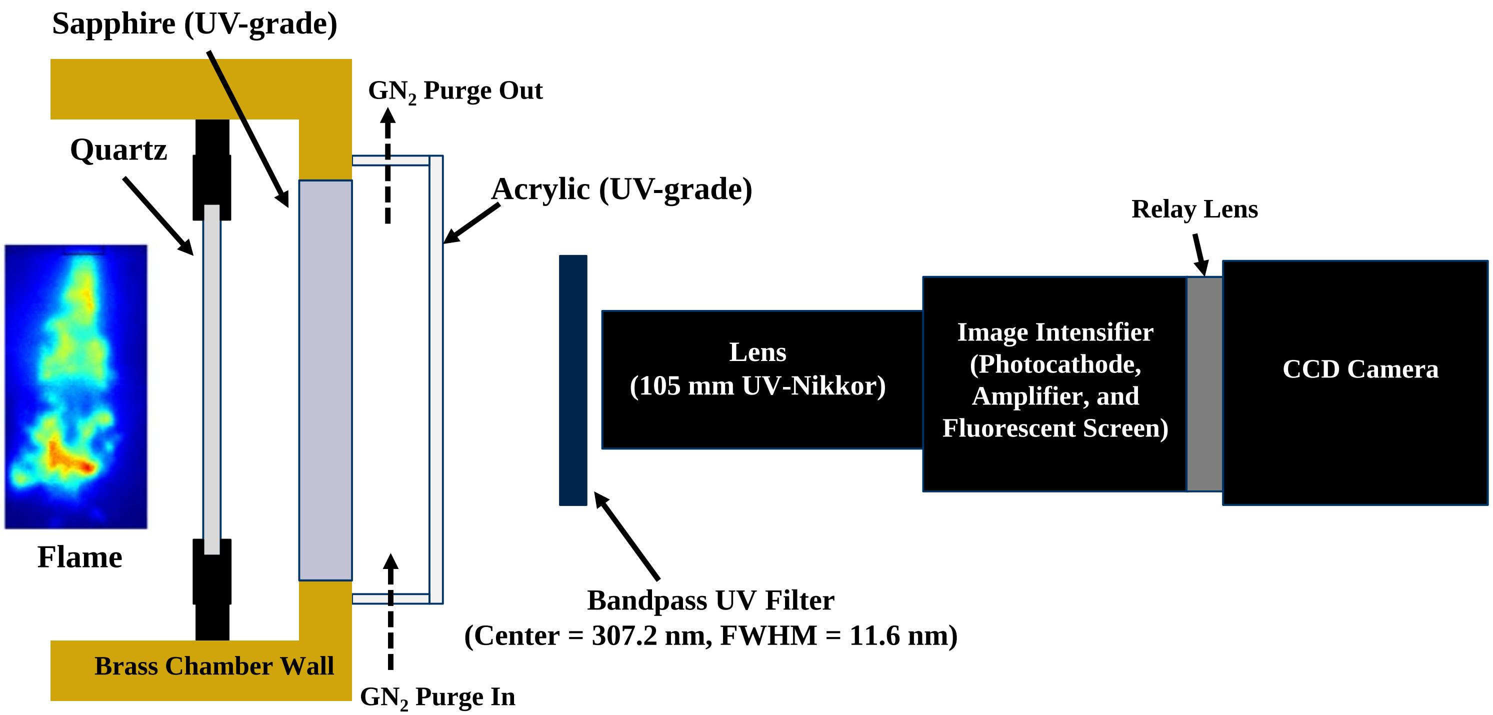

- **Unwanted radiation from vibrational and rotational bands of H_2O products are not recorded.**
- **Nitrogen purge removes condensation from window surfaces.**

Experimental Techniques: Test Matrix

Convective Shear Layer Velocity by Dimotakis [*AIAA*, 1986][5]

- Vortex Frame of Reference

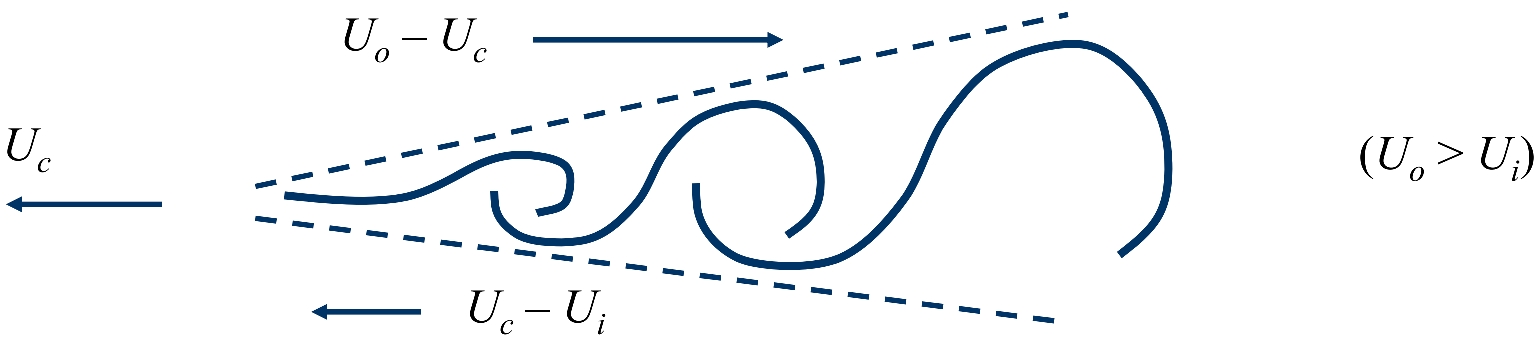

- Bernoulli's equation
  - A stagnation point must exist between vortices. Therefore, along a line through this point, dynamic pressures are approximately equal.

$$\rho_o (U_o - U_c)^2 \approx \rho_i (U_c - U_i)^2$$

$$U_c = \frac{U_o \rho_o^{1/2} + U_i \rho_i^{1/2}}{\rho_o^{1/2} + \rho_i^{1/2}}$$

$$St = \frac{f_{nat} D}{U_c}$$

$\Rightarrow$ If *St, D,* U_c are held constant then f_{nat} may be constant.

[5] Dimotakis, P. E. 1986 "Two-Dimensional Shear-Layer Entrainment," *AIAA J.* 24, 1791-1796.

Experimental Techniques: Heat Exchangers

- Outer Jet Heat Exchanger

(data collected using helium)

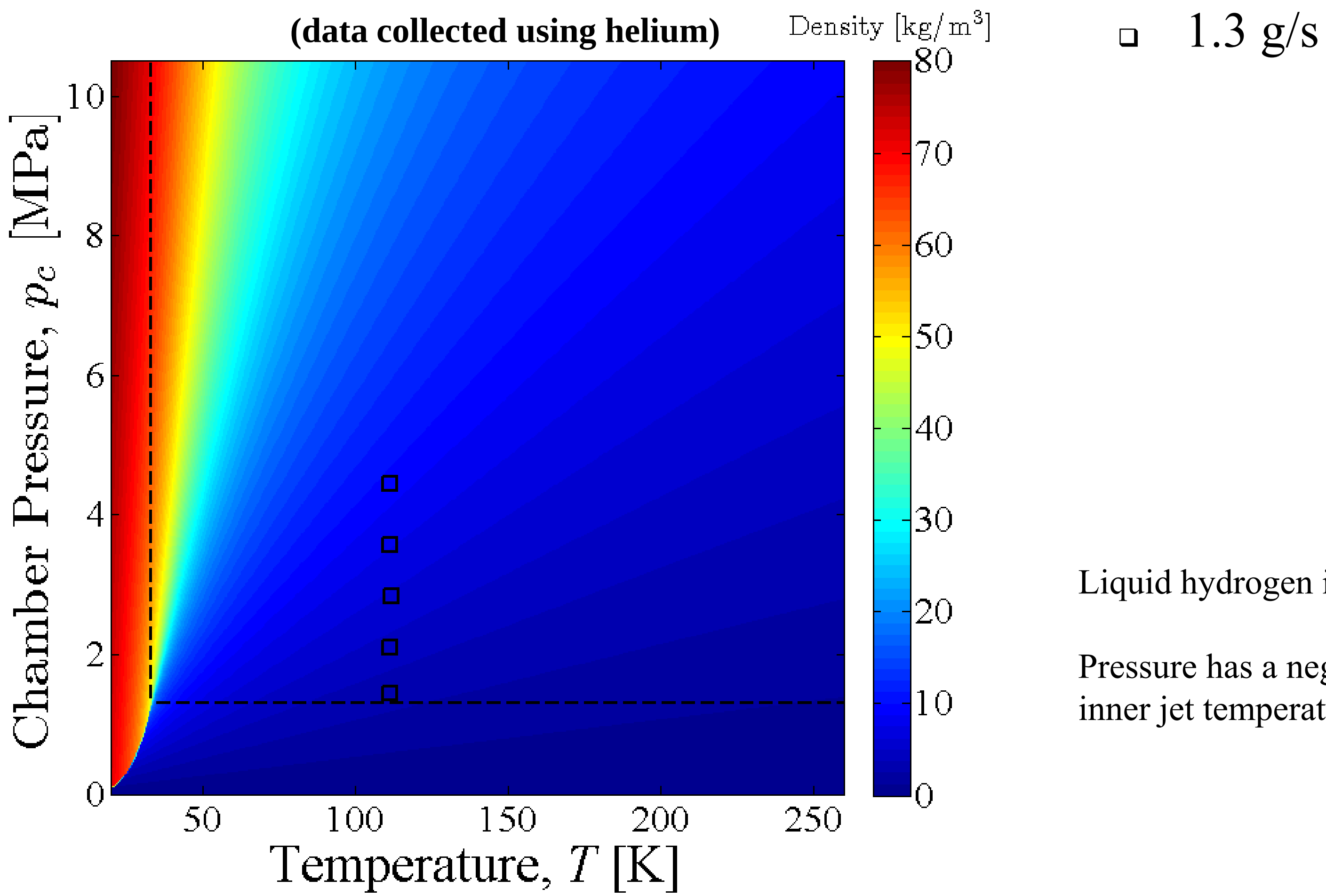

Liquid hydrogen is unachievable.

Pressure has a negligible effect on inner jet temperature.

Results: Unforced Coaxial Jets

- Natural Jet Characterization: *St* scaling law produced by **theoretical** shear layer convection velocities

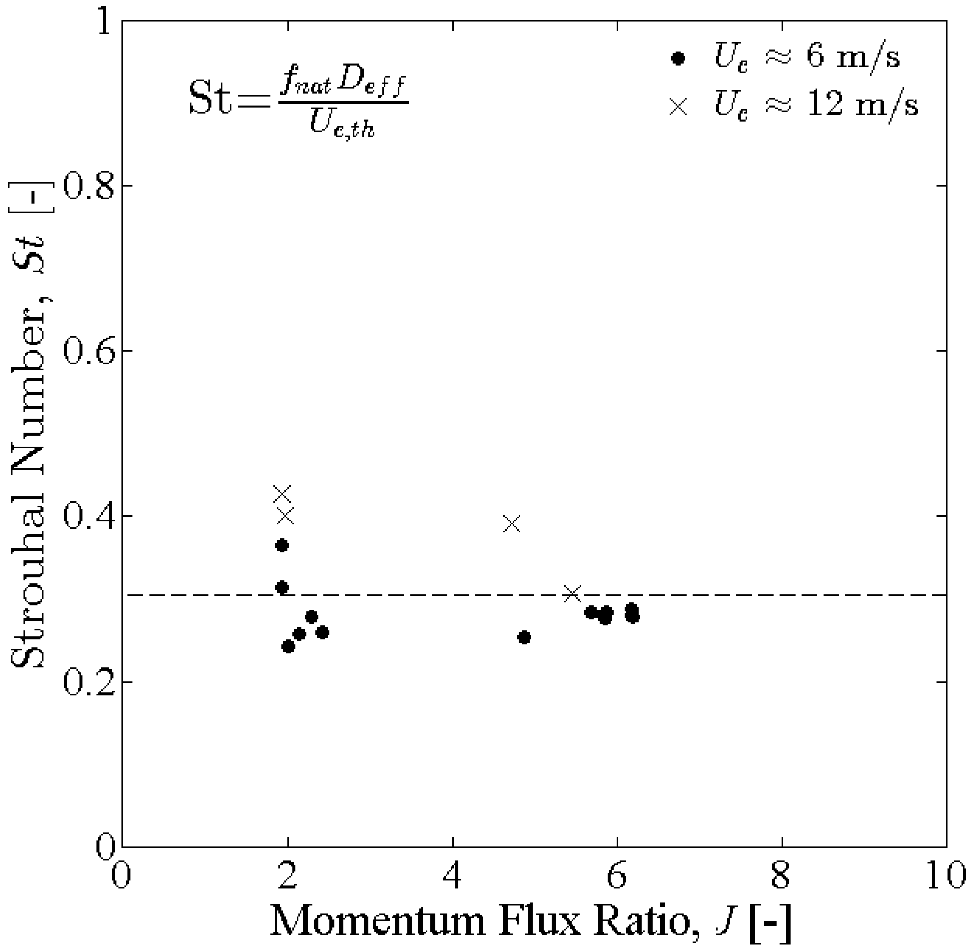

- $D_{eff} = \dfrac{D_1+D_2}{2}$

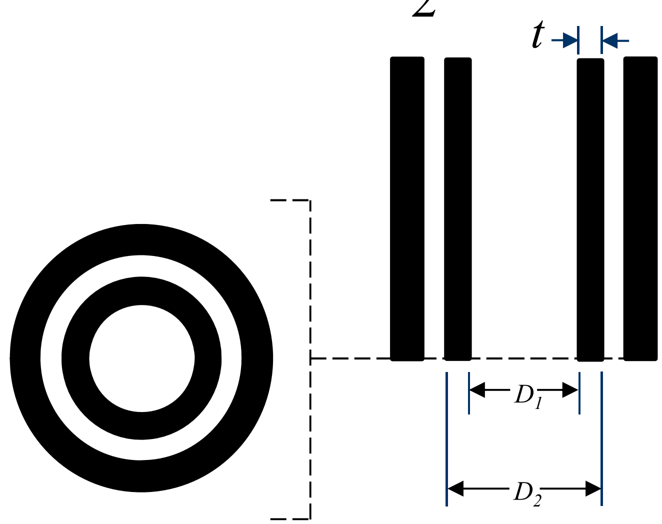

⇨ *St* values have a mean of 0.30

⇨ *St* is not dependent on *J*

⇨ High shear layer convection velocities show more scatter